OPEN ACCESS

Environment & Ecology ARTICLE

Eutrophication-driven widespread surface dissolved oxygen enrichment in Chinese lakes: A warming-vulnerable transient state?

Yindong Tong,[1,2] Feng Zhao,[1] Zhao Huang,[1] Qirui Wang,[1] Xiangzhen Kong,[3,4,*] Wei He,[5] Yan Lin,[6] Lei Chen,[7] Erik Jeppesen,[8,9,10] Robert Ladwig,[9] Yue Qin,[11] and Yong Liu[11,*]

*Correspondence: xzkong@niglas.ac.cn (X.K.); yongliu@pku.edu.cn (Y.L.)

Received: October 9, 2025; Accepted: March 24, 2026; Published Online: March 30, 2026; https://doi.org/10.59717/j.xinn-geo.2026.100215

GRAPHICAL ABSTRACT

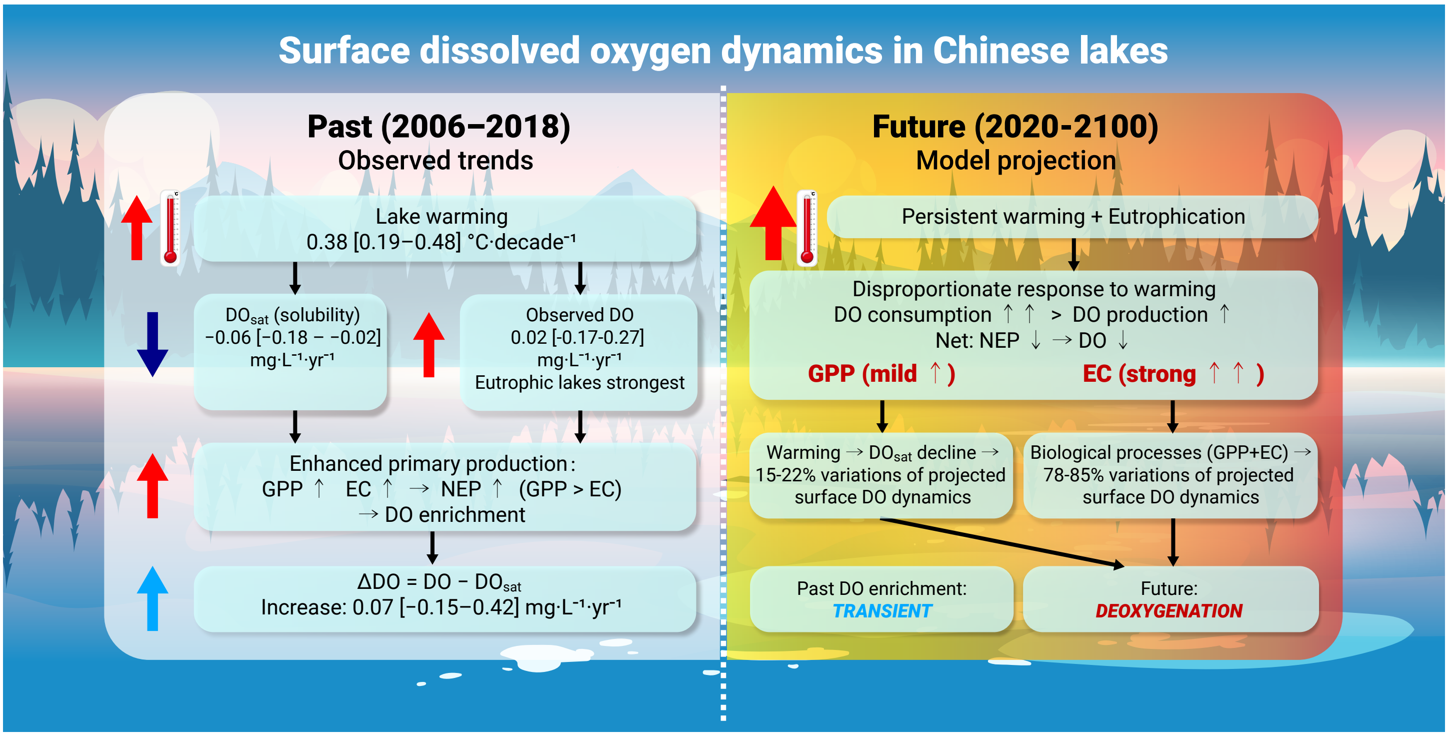

PUBLIC SUMMARY

- Dissolved oxygen increased in ~100 Chinese lakes with a rate of 0.07 (-0.15–0.42) $mg \cdot L^{-1} \cdot yr^{-1}$ (2006–2018).
- DO enrichment was most pronounced in eutrophic lakes, primarily driven by elevated primary production.
- Future projections suggest rising nutrient loads reverse the lake DO enrichment and lead to deoxygenation.

Eutrophication-driven widespread surface dissolved oxygen enrichment in Chinese lakes: A warming-vulnerable transient state?

Yindong Tong,[1,2] Feng Zhao,[1] Zhao Huang,[1] Qirui Wang,[1] Xiangzhen Kong,[3,4,*] Wei He,[5] Yan Lin,[6] Lei Chen,[7] Erik Jeppesen,[8,9,10] Robert Ladwig,[9] Yue Qin,[11] and Yong Liu[11,*]

[1]School of Environmental Science and Engineering, Tianjin University, Tianjin 300072, China
[2]School of Ecology and Environment, Tibet University, Lhasa 850000, China
[3]State Key Laboratory of Lake and Watershed Science for Water Security, Nanjing Institute of Geography and Limnology, Chinese Academy of Sciences, Nanjing 211135, China
[4]Helmholtz-Centre for Environmental Research-UFZ, Department Lake Research, Magdeburg 39114, Germany
[5]School of Water Resources and Environment, China University of Geosciences (Beijing), Beijing 100083, China
[6]College of Environmental Science and Engineering, Nankai University, Tianjin 300350, China
[7]State Key Laboratory of Water Environment Simulation, School of Environment, Beijing Normal University, Beijing 100875, China
[8]Institute for Ecological Research and Pollution Control of Plateau Lakes, School of Ecology and Environmental Sciences, Yunnan University, Kunming 650500, China
[9]Department of Ecoscience, Aarhus University, Aarhus 8000, Denmark
[10]Sino-Danish Centre for Education and Research, Chinese Academy of Sciences, Beijing 100101, China
[11]College of Environmental Sciences and Engineering, State Environmental Protection Key Laboratory of All Material Fluxes in River Ecosystems, Institute of Tibetan Plateau, Peking University, Beijing 100871, China
*Correspondence: xzkong@niglas.ac.cn (X.K.); yongliu@pku.edu.cn (Y.L.)

Received: October 9, 2025; Accepted: March 24, 2026; Published Online: March 30, 2026; https://doi.org/10.59717/j.xinn-geo.2026.100215

Citation: Tong Y., Zhao F., Huang Z., et al. (2026). Eutrophication-driven widespread surface dissolved oxygen enrichment in Chinese lakes: A warming-vulnerable transient state? *The Innovation Geoscience* **4**:100215.

Dissolved oxygen (DO) is a critical determinant of lake ecosystem function and services. The interaction between climate warming and anthropogenic nutrient inputs exerts opposing effects on lake DO—warming decreases gas solubility (DO_{sat}), while nutrient enrichment enhances net ecosystem production through eutrophication-driven primary production, potentially leading to transient DO enrichment. This creates a vulnerable state that may shift under future climate-nutrient interactions, which limits accurate predictions of lake DO dynamics. Here, we calculated ΔDO (= DO – DO_{sat}) in the surface waters of 99 freshwater lakes in China (66 subtropical and 33 temperate), spanning a broad trophic gradient (TN: 0.1–8.3 mg·L^{-1}; TP: 5.4–256 μg·L^{-1}). Using a combined process-based and data-driven modeling approach, we examined DO dynamics in relation to water temperature, primary productivity, and water quality. Despite rapid lake warming (0.38 [0.19–0.48]°C·decade^{-1}) and a corresponding decline in DO_{sat} (-0.06 [-0.18 – -0.02] mg·L^{-1}·yr^{-1}), we observed widespread DO enrichment from 2006 to 2018, with an average ΔDO increase of 0.07 [-0.15–0.42] mg·L^{-1}·yr^{-1}. This enrichment was most pronounced in eutrophic lakes, driven by enhanced primary production. However, future projections suggest that current DO enrichment trends may be a transient state and reverse due to a disproportionate increase in DO consumption relative to production, driven by asymmetric responses to warming, potentially leading to deoxygenation. While nutrient management is widely regarded as an effective strategy against eutrophication, our findings underscore the need to carefully assess its coupled effects on lake DO before implementation. Given the accelerating warming of water bodies, developing nutrient management strategies informed by lake DO levels should be a priority.

INTRODUCTION

Dissolved oxygen (DO) in aquatic ecosystem affects biodiversity,[1] nutrient biogeochemistry,[2] greenhouse gases emission,[3] drinking water qualities,[4] and ultimately, human health.[5] With climate warming intensively affecting lake ecosystem, a well-acknowledged consequence is the recorded continuous and rapid rising of surface water temperatures worldwide.[6,7] Rising temperature could result in the reduced oxygen solubility, which has been proposed to be a dominant responding factor for the recently deoxygenation in the global lakes.[1,8,9] Despite that deoxygenation has previously been reported in the coastal and ocean water since the middle of the 20th century,[10] a recent study have shown a 2.8–9.3 times greater DO decline in lakes located in developed countries, than in the ocean.[1]

Climate warming and high nitrogen and phosphorus inputs promote phytoplankton growths and the formation of, potentially, harmful algal blooms, posing a profound impact on freshwater ecosystems,[11,12] particularly prominent in the developing countries where management of nitrogen and phosphorus discharge remains extensive but presently seems to be insufficiently effective.[13,14] Global increase of lake algal blooms has been evidenced since the 1980s,[11] and the trend is anticipated to expand at both scales and intensities due to the climate warming.[13] Over 40% of global lakes exhibit eutrophic conditions, with nutrient-driven chlorophyll-a increases particularly pronounced in densely populated regions. Chinese lakes show much higher nutrient-to-chlorophyll conversion efficiencies than global averages, reflecting both intensive agricultural inputs and warmer temperatures accelerating primary production.[15,16]

Phytoplankton could play dual roles in regulating DO concentration in freshwater ecosystem.[17] Phytoplankton proliferation can induce pronounced dissolved oxygen (DO) supersaturation (~95%–150%) via photosynthesis, yet subsequent bloom degradation generates autochthonous organic matter that drives DO depletion through microbial mineralization.[17] Critically, asymmetric temperature sensitivities in aquatic production versus consumption processes may further destabilize DO dynamics under climate warming.[18] This complex nexus—where warming simultaneously stimulates phytoplankton growth and accelerates respiratory consumption—hinders accurate DO prediction. Compounding this uncertainty, inadequate nutrient management in developing economies has intensified the dual pressures of eutrophication and thermal forcing in freshwater lakes,[14,19] despite the persistent knowledge gap in disentangling these drivers' relative contributions to DO variability.

To characterize the trend of DO concentrations in the lakes of different trophic status and key drivers of DO variations, we compiled an extensive dataset for 99 freshwater lakes across China (66 subtropical lakes and 33 temperate lakes) (Figure 1). Most lakes are shallow, with a median depth of 5.7 m. DO in the surface water (0.5 m below the surface) was analyzed together with the primary productivity (using chlorophyll-a as a proxy), nutrient concentrations, and climates, including air/surface water temperatures, wind speeds, and solar radiation in 2018. Among these lakes, 50 with continuous and monthly data during 2006–2018 were studied in more details. A sequential approach of process-based model (i.e. PCLake+) and statistical analysis (i.e. general linear model, GLM and Random Forest algorithm, RF) was used to identify the major drivers for historical changes in lake DO and to perform future projections under different climate and nutrient loading scenarios (Figure 1). Combining a model approach with the long-term (2006–2018) and monthly lake water quality data analysis covering a large gradient of climate and trophic status across the nation allows us to quantify the complex nexuses of warming and productivities on long-term lake DO dynamics, to refine the prediction of the feedback between lake DO and climates, and to better inform future nutrient management. We specifically address the two hypotheses below: (1) The observed trends in DO levels in

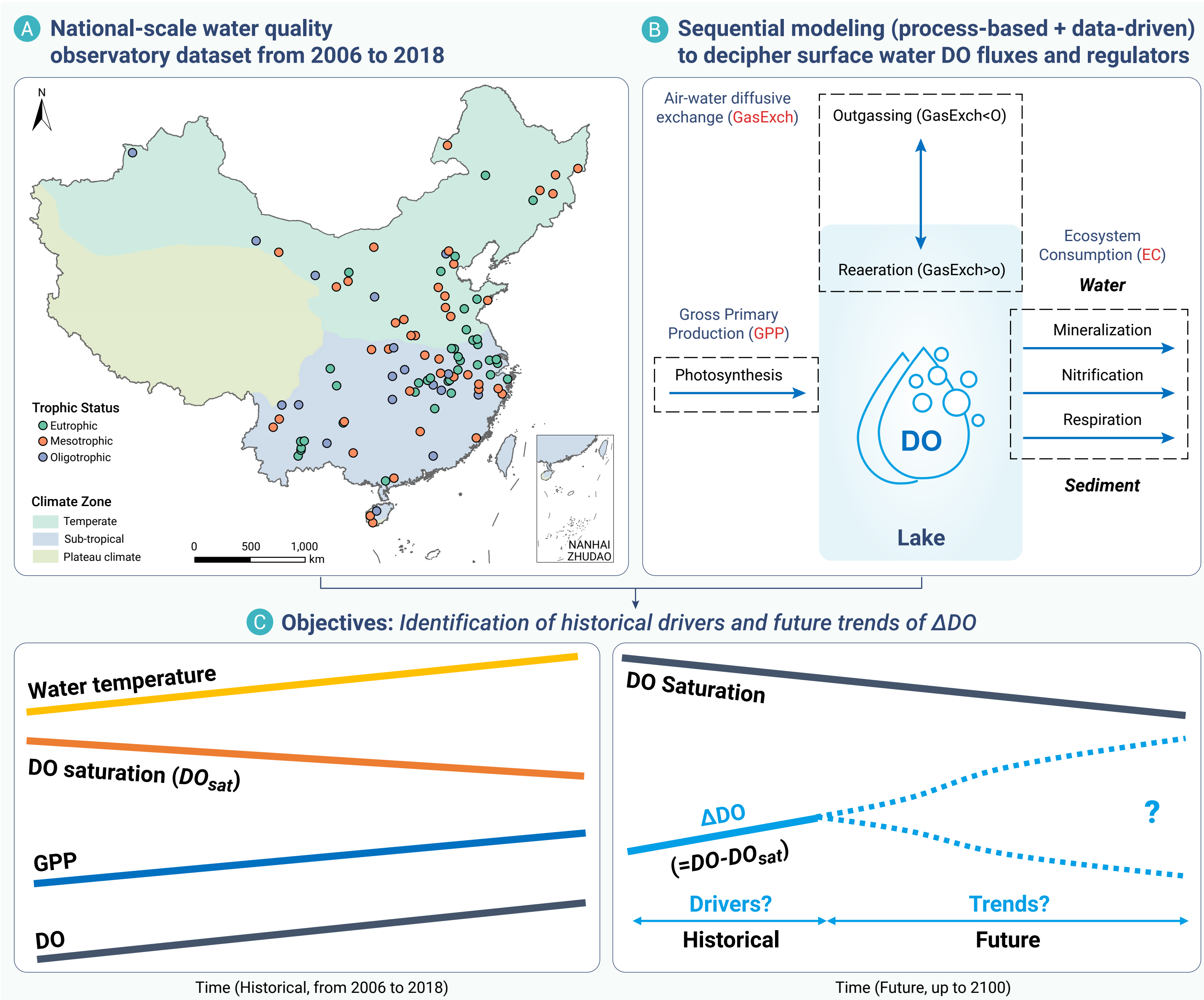

Figure 1. Conceptual diagram of workflow, including (A) lake monitoring dataset, (B) sequential modeling, and (C) hypothesis and objectives A long-term (2006–2018) monthly water quality observation dataset for lakes surface water across China was compiled. A sequential process-based and data-driven modeling was developed to decipher the regulators of DO in the historical period (2006–2018) and to project their future trends. ΔDO is defined as DO-DO_{sat}, so that ΔDO = 0 denotes 100% DO saturation. Among all the 99 studied lakes, 66 were in the subtropical region, while the other 33 lakes were situated in the temperate region.

the studied lake surface water (2006-2018) were primarily driven by increased primary productivity associated with eutrophication. (2) Future trends in lake DO levels may reverse leading to deoxygenation due to asymmetric increases in gross primary production and ecosystem respiration, resulting in a shift from positive to negative net ecosystem productivity.

MATERIALS AND METHODS

Water quality monitoring data

We obtained an extensive surface water quality monitoring dataset including the years 2006 to 2018 from the National Water Quality Monitoring Program in China,[20] with ambitions of creating unbiased assessments of water quality in freshwater lakes across the country. They were based on the randomized, unequally weighted probability surveys overseen by the Ministry of Ecology and Environmental Protection, China, with the goal of creating unbiased assessment of water qualities in freshwater lakes across China. The number of monitoring sites for each lake depends on its surface area. Generally, for the lakes with a surface of 50–100 km^2, around 3–5 sampling sites were monitored. For lakes with a surface area > 100 km^2, more than 5 sites were monitored. Most of these lakes surveyed are shallow, with a median depth of only 5.5 m. During the whole study period, the standard of sampling site selection and procedure of water collections are consistent, which were based on the "Technical Specifications Requirements for Monitoring of Surface Water and Wastewater in China". This approach allowed us to analyze and compare water quality trends more effectively.

Our dataset addresses two core objectives: (a) characterizing 2018 national lake ecological status, and (b) quantifying 2006–2018 temporal trends (Dataset S2). The dataset includes 99 freshwater lakes (301 monitoring sites) across 29 Chinese provinces in 2018, covering diverse ecological zones (e.g., temperate northern and subtropical southern lakes). It contains monthly measurements of key water quality parameters (i.e., DO, chlorophyll-a [Chl-a], total nitrogen [TN], total phosphorus [TP], NH_4^+-N, COD_{Mn}, Secchi depth [SD], and water temperature) and lake morphometric attributes (location, surface area, depth, volume). The dataset was chosen for cross-sectional analysis due to its unparalleled spatial coverage, enabling robust regional inferences on eutrophication and pollutant distribution. In addition, 50 of these 99 lakes (204 sites) with continuous 2006–2018 monthly data were available to assess long-term DO trends and drivers. The combined datasets provide sufficient statistical power to parameterize models (PCLake+) and disentangle drivers of lake DO dynamics.

The DO saturation (DO_{sat}) in these lakes was calculated from the monitored water temperature and calibrated by the lake altitude.[21] ΔDO was estimated as difference between DO and DO_{sat} concentration. A positive ΔDO signifies DO oversaturation, and a negative ΔDO represents DO undersaturation or DO deficit. We characterize the trend of water quality indexes based on the regression analysis between the monthly water quality data and corresponding sampling time. The slope (k) in the regressions was defined as the monthly increase rate (if $k > 0$) or decrease rate (if $k < 0$) during the study period. Information on surface area, mean depth, and water volume in the lakes was derived from the HydroLAKES provided by the Global HydroLab.[22] To identify potential drivers of water temperature change, we also collected monthly climate data from ERA5-Land by the European Centre for Medium-Range Weather Forecast including wind speed, solar radiation, precipitation, and air temperature for the period of 2006–2018.[23]

Chemical analysis of water quality variables in lakes

The procedures applied for selecting the sampling sites in lakes and collecting water samples were generally consistent throughout the study period and based on the technical requirements for monitoring of surface waters in China. Given that most of the surveyed lakes in our study were shallow with a median depth of 5.5 m, we collected surface water samples at a depth of 0.5 m below the lake surface. This sampling approach was employed to capture representative water quality data from the upper layer of lakes where the key biological and chemical processes occur. Standard methods were applied for measuring nutrients, COD_{Mn}, and Chl-a concentrations. An unfiltered aliquot of lake water was prepared for each sample. TN concentrations were measured by the persulfate digestion, followed by colorimetric analysis (N-[1-naphyl] ethylene diamine dihydrochloride spectrophotometry), with a method detection limit (MDL) of 50 μgN·L^{-1}.[24] TP concentrations were determined by persulfate digestion, followed by automated colorimetric analyses (ammonium molybdate and antimony potassium tartrate under the acidic condition), with an MDL of 10 μg·L^{-1}. The COD_{Mn} was determined using the conventional permanganate method ($KMnO_4$), with an MDL of 0.5 mg·L^{-1}. Raw water was filtered by filter membranes for measurements of Chl-a and NH_4^+-N concentrations. NH_4^+-N concentration is determined by flow injection analysis and salicylic acid spectrophotometry with an MDL of 10 μg·L^{-1}. Chl-a in the water was extracted by acetone and determined by spectrophotometry with an MDL of 1 μg·L^{-1}. Transparency was determined as the Secchi depth (SD) with an MDL of 0.1 cm. The other surface water quality variables (i.e. DO concentration and water temperature) were measured using multiparameter water quality sensors with the MDLs of 0.01 mg·L^{-1} and 0.01°C for DO and water temperature, respectively.

Sequential modeling approach: Part #1

Process-based modeling of lake DO with PCLake+. To identify the drivers for DO enrichment, we applied a process-based modeling approach based on the aquatic ecosystem model PCLake+.[25] The PCLake+ model is a well-developed lake ecosystem dynamical model with a hypolimnion layer so that the model can be used to a wide range of freshwater lakes that differ in depth and stratification regime.[25,26] PCLake+ incorporates key biogeochemical processes that are determinant for lake DO in water and sediments (Figure 1 & Table S1): (1) air-water diffusive exchange (GasExch, both outgassing and reaeration), (2) ecosystem consumption (EC; mineralization, nitrification and respiration in water/sediment), and (3) gross primary production (GPP; both phytoplankton [GPP_P] and macrophytes [GPP_M]). These processes are summarized by equations (1-3):

$$\frac{\partial DO}{\partial t} = NEP + A + E = GPP + EC + A + E \tag{1}$$

$$NEP = GPP + EC \tag{2}$$

$$GPP = GPP_P + GPP_M \tag{3}$$

where NEP is net ecosystem production, A is the atmospheric exchange, GPP is gross primary production (which can be further split into GPP by phytoplankton and by macrophytes), EC is ecosystem respiration (always a negative sink term), and E is external loads of oxygen (e.g., the hydrologic exchange) or internal sink like diffusion into sediment. Further, the model has been modified to represent the lower DO_{sat} in lakes at high elevations in the present study (Text S1). Besides, PCLake+ model embraces key ecological concepts, including closed cycles of substances (i.e., carbon, nutrient, and matter), food-web dynamics, and trophic cascade. The model parameters had been calibrated against the field data from over 40 lakes[26-28] and were widely utilized for China's lakes.[26,29] For a full description of the PCLake+ model and its parameter set, we refer to references.[25,27]

Boundary conditions and model configurations. We ran the PCLake+ model for the 50 lakes in the database with long-term monthly water monitoring data from 2006 to 2018. To increase the representativeness of oligotrophic lakes, we included 12 additional oligotrophic lakes with data available in 2018. Thus, a total of 62 lakes were included in the model simulations (i.e., 24 eutrophic, 20 mesotrophic, and 18 oligotrophic lakes). Basic parameters for these lakes as the inputs to the model were obtained from the LakeAtlas database,[22] including coordinates, lake fetch (square root of surface area), average depth, elevation, sediment property (clay fractions, organic carbon content, dry weight), discharge, and evaporation. The daily water temperature data for epilimnion were obtained from the global database,[6] including the historical periods from 1981 to 2020 and future projection periods from 2006 to 2099. PCLake+ estimated lake mixing depth according to the empirical relationship as function of fetch and depth, and considered the lake as stratified if the mixing depth is lower than the depth.[25] In addition, daily incoming radiation was calculated using an embedded function in PCLake+ based on the lake latitude.[25]

Given the difficulty in obtaining the detailed nutrient loading data for each lake during the simulation period, we employed an alternative method to a "back-calculate" nutrient loading for each lake based on the model simulations and observations. Specifically, we ran the model for each lake in two steps. First, the model was run for each lake with a default and constant nutrient loading derived from the global average level (i.e., TN load: 0.025 g N m^{-2} per day; TP load: 0.0025 g P m^{-2} per day).[30] Then, we estimated the nutrient load to the lake based on in-lake nutrient concentration. Simulated TN and TP concentrations were used for comparison with observed data, and a correction factor for the nutrient load was calculated as: $NutCorr_{n,i,t} = \frac{Obs_{n,i,t}}{Mod_{n,i,t}}$, where n denotes either nitrogen or phosphorus, i denotes the lake index, and t denotes the time. Then, the model was re-run for each lake with $NutCorr_{n,i,t}$ as an additional input to adjust the nutrient loadings during each time step of the simulation period. We considered $NutCorr_{n,i,t}$ as a 'scaling factor' of the 'calibrated' nutrient load, thus the model can substantially increase the accuracy in tracking the long-term dynamics of the in-lake nutrient concentration, thus providing a sound basis for DO predictions. Note that other water quality data such as the DO concentration are not used in this procedure.

Historical simulation and Bayesian calibration. For each of the 62 lakes, the model simulated the daily DO dynamics for the historical period from 1981 to 2018. The period from 1981 to 2005 was considered as the 'spin-up' stage of the simulation while the model outputs from 2006 to 2018 were applied for model calibrations. The nutrient loading for each month during 2006 to 2018 was corrected values based on the back-calculation method as described above. For the spin-up period from 1981 to 2005, the average nutrient loading from 2006 to 2018 was adopted. Lake basic parameters and water temperatures were fed into the models for each lake. Model predictions were compared with the field data on DO and ΔDO.

We performed a Bayesian calibration on the model parameters for each of the 62 modeled lakes.[27] Before the calibration, the model parameters had adopted the default values derived from previous calibrations against 40+ lakes.[27] A subset of parameters was selected for the Bayesian calibration according to the sensitivity analysis.[27,28] A total of 12 parameters considered sensitive in modeling DO dynamics and showing profound variability among lakes were selected (Table S2). An additional 6 parameters were included in the calibrations since they are linked to the 12 parameters above, leading to a total of 18 parameters for Bayesian calibration.

The procedure of Bayesian calibration was composed of three steps below (see Figures S15-S16 for the workflow chart and the posterior distribution of

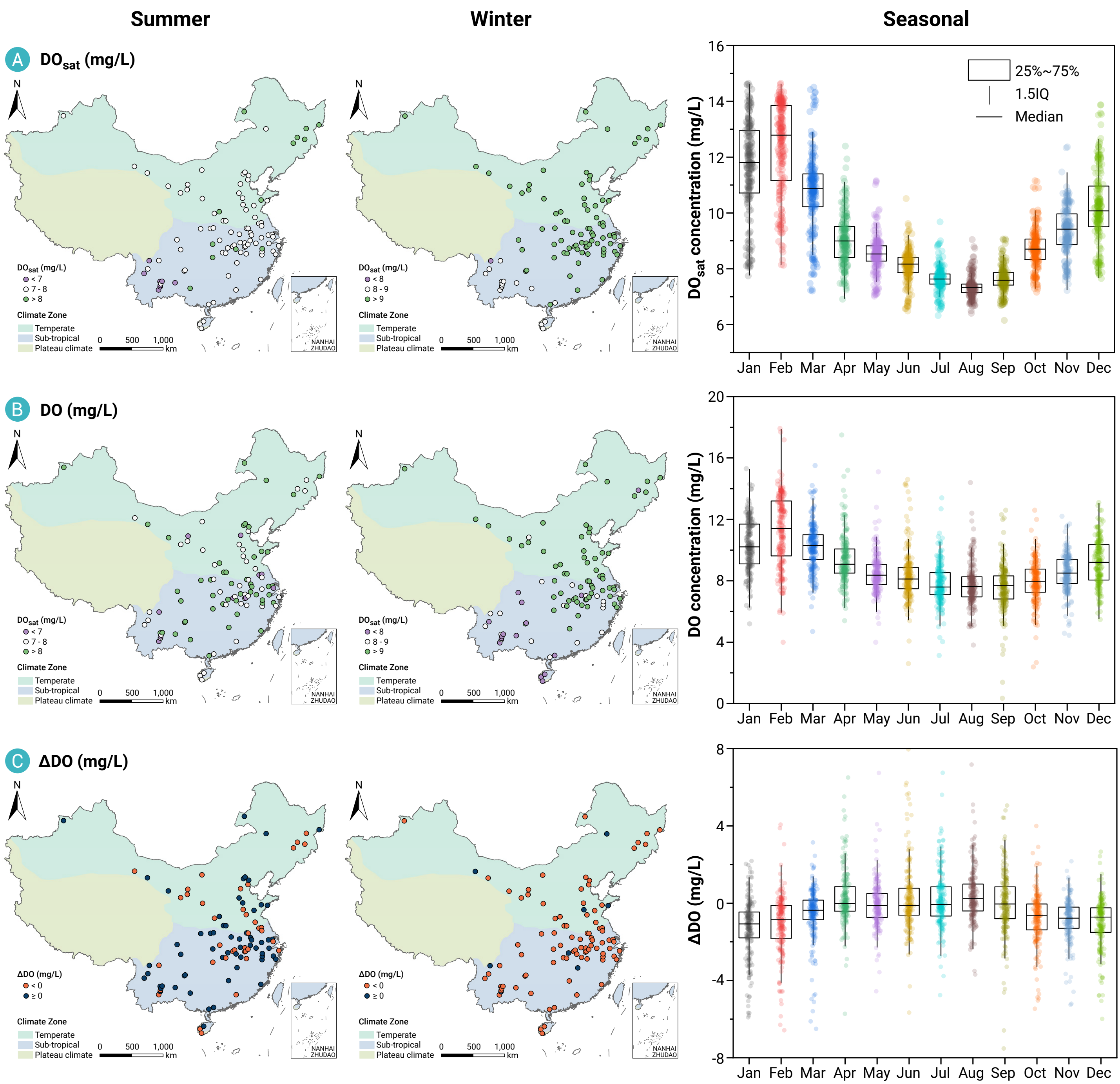

Figure 2. Spatial versus temporal patterns of (A) DO_{sat}, (B) DO, and (C) ΔDO in freshwater lakes across China A positive ΔDO represented a DO oversaturation and a negative represents deficit. Here, two thirds of the 99 lakes display DO oversaturation in summer while only seven lakes display DO oversaturation in winter.

the parameters):

(1) Parameter_space. For selected k (= 12) parameters, theoretical ranges are determined based on the literature and a grid sampling is created, i.e., every parameter takes different p values. Then, a database space for selected parameters (*parameter_space*) is established with k by p grid. Here we used p = 8, which is considered sufficient for the purpose.[27]

(2) Parameter_pool. Based on *parameter_space*, the Morris method is adopted, and a pool of parameter combination (*parameter_pool*) is created with r samples. For each parameter in each sample, the value is randomly selected from *parameter_space*, i.e. among the p values. Here we used r = 20, which is considered sufficient for the purpose.[27] The default parameter set is added as an extra sample so that the *parameter_pool* contains r+1 samples in total.

(3) Parameter_db. The model is run with each of the parameter combinations in *parameter_ pool*, and for each run likelihood is calculated based on the squared residuals of the natural logarithms of the observed and simulated values after adding a small value (Equation 4; ε, 'minimum significant difference').

$$\phi_{i,j} = \left[log\left\{ \frac{(y_{j,obs}+\varepsilon_j)}{(y_{j,sim}+\varepsilon_j)} \right\} \right]^2 \qquad (4)$$

where $\phi_{i,j}$ denotes the fitting function, i is the sample index (i = 1,2,...,r), and j is the water quality variable (here only DO concentration is applied). The ε value is chosen as powers of e (7.4 mg·L^{-1} for DO). The $\phi_{i,j}$ value ranges from 0 (prefect fit) to 20 (very bad fit), and a value of 1.0 means a difference factor e (2.72) between the observed and simulated data. For each lake, the parameter combination with the lowest $\phi_{i,j}$, or the maximum likelihood among all (r +1) samples, is considered as the best run and selected as the calibrated

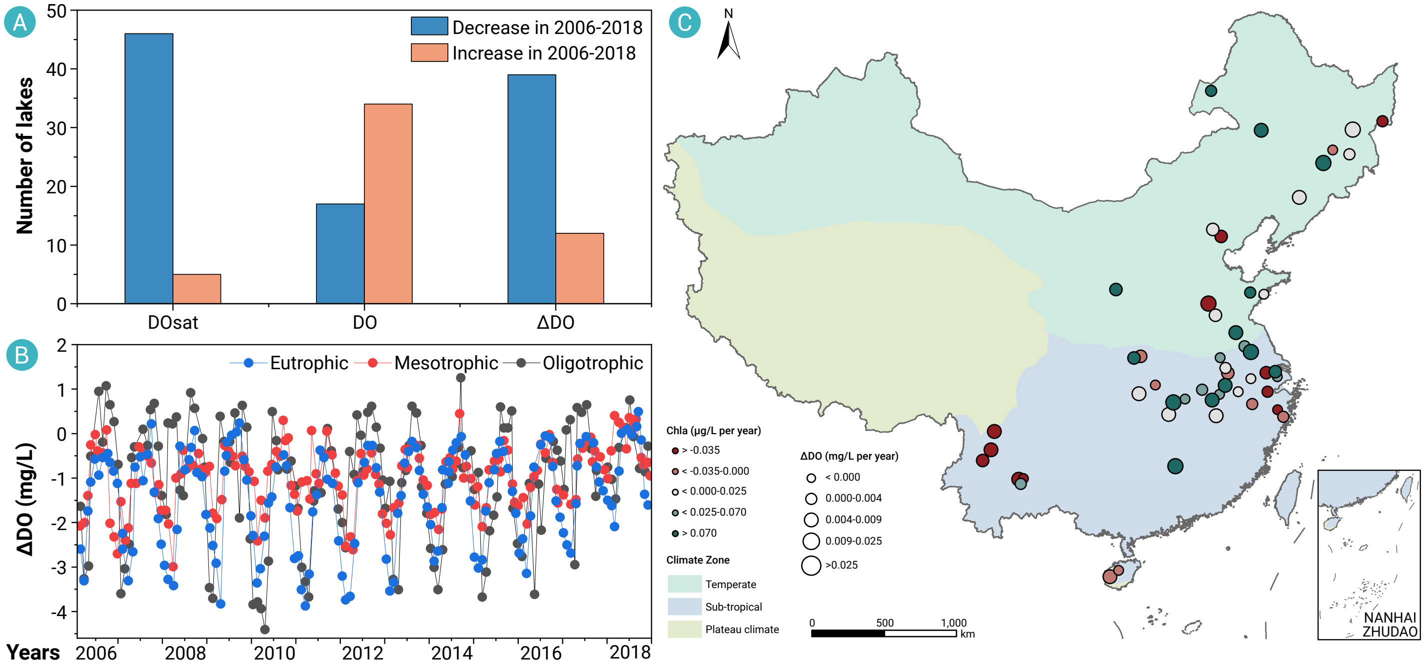

Figure 3. Trends of DO concentrations in China's freshwater lakes (n = 50) during 2006–2018 (A) The number of lakes with different trends in DO_{sat}, DO, and ΔDO; (B) Monthly variations of ΔDO during the study period; (C) Trends of Chl-a concentrations and ΔDO values in the investigated lakes. Lakes with higher Chl-a increasing trends tend to show higher ΔDO increasing trends (Figure S4).

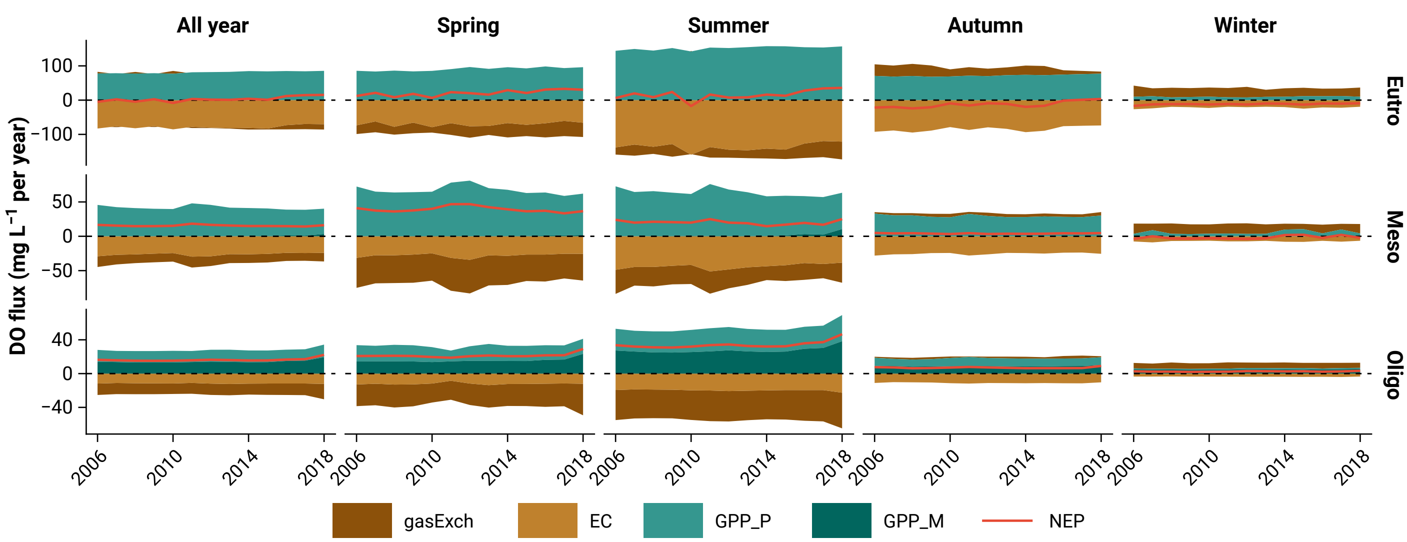

Figure 4. Modeled DO fluxes of various process groups during 2006–2018 in different seasons and lakes with distinct trophic states using the PCLake+ model The values were the average values of modeled lakes within each group. Positive values denoted an input DO flux to the water column, and a negative value referred to the loss DO flux. NEP denotes the net ecosystem production (i.e., $GPP_M + GPP_P - EC$). GPP_M and GPP_P represent the gross primary production from macrophytes and phytoplankton, respectively. EC denotes the ecosystem consumption (mineralization, nitrification and respiration in water/sediment). gasExch denotes the air-water oxygen diffusive exchange including both outgassing and reaeration. "Eutro", "Meso", and "Oligo" represent eutrophic, mesotrophic and oligotrophic lakes, respectively. Detailed definitions of these process groups were provided in Table S1.

parameter set, which is used for model simulation and future projection for that specific lake. Calibrated parameter sets for all the lakes constitute *parameter_db*.

The model showed a good fit of the simulated DO with the field data across various lakes (Figures S17-S18) and was a significant improvement after the Bayesian calibration.

Future projections. We performed a future projection for the 62 lakes under different climate warming and nutrient loading scenario. Specifically, projections for the daily water temperature for both epilimnion and hypolimnion from 2006 to 2099 were derived from a global database,[6] estimated by the FLake model driven by four Global Climate Models (i.e., HadGEM2-ES, IPSL-CM5A-LR, MIROC-ESM-CHEM, and GFDL-ESM2M) of three typical Representative Concentration Pathways (i.e., RCPs 2.6, 6.0, and 8.5), resulting in 12 runs for each lake for climate projection.

In addition, we designed two nutrient loading scenarios (nutrient (+) and (-), applied to both TN and TP). For the 2006–2018 modeling spin-up period, nutrient loading was set to the average value from the 2006–2018 calibration period. Building on the nutrient loading change rates for China's lakes during 2006–2018,[31,32] we simulated nutrient loading dynamics from 2019 to 2099 by applying a realistic monthly change rate of ± 0.1%. This incremental adjustment over the 80-year period yields two ecologically relevant scenarios: a cumulative reduction of 62.3% (nutrient (-)), reflecting the potential long-term impacts of sustained nutrient abatement policies (e.g., wastewater treatment upgrades, agricultural runoff control); and a +264% increase (nutrient (+)), driven by unmitigated nutrient input growth from population expansion, intensified agriculture, or weakened environmental regulation, the trends

Table 1. Correlation analysis and general linear model of trends in the monitored DO and DO saturation (DO_{sat}) from 2006 to 2018.

Variables	DO in the lakes				ΔDO in the lakes			
	R	*P*	*Beta*	*RI%*	*R*	*P*	*Beta*	*RI%*
Chl-a	0.281	0.001	0.373	63%	0.379	0.013	0.401	53%
COD_{Mn}	-0.032	0.704	-0.013	1%	0.061	0.463	-0.059	1%
Water temp.	-0.007	0.936	-0.104	3%	0.299	0.000	0.179	27%
Secchi depth	-0.129	0.118	0.002	7%	-0.143	0.037	0.002	5%
Total Nitrogen (TN)	-0.098	0.238	0.091	4%	0.047	0.575	0.149	3%
Total Phosphorus (TP)	-0.159	0.054	0.091	9%	-0.006	0.942	0.259	3%
NH_4^+-N	-0.145	0.078	-0.353	14%	-0.039	0.040	-0.478	9%

*Beta: Standardized coefficient value in the GLM models; RI: Relative Influence (%).

consistent with historical nutrient loading trajectories in unmanaged lake basins. The PCLake+ model projects DO, DO_{sat}, and ΔDO, and the relevant processes for DO dynamics as described above.

Sequential modeling approach: Part #2

Statistical analyses using multi-variant models. The 50 lakes with continuous water quality monitoring data for 2006–2018 were selected for statistical analysis. Prior to the analysis, we used linear regression to characterize the temporal trends in water quality for each lake monitoring station between 2006 and 2018. Slopes of linear regressions for DO and ΔDO were applied as response variables, and the explanatory variables included the changes of other water quality indexes (i.e., TN, TP, and NH_4^+-N) over the years. Then, we used general linear model (GLM) and redundancy analysis (RDA) to identify potential linear relationships between the monitored DO concentrations (or ΔDO) and other water quality data (e.g., Chl-a, SD, water temperatures, and nutrients) and to quantify their relative contributions to DO dynamics. RDA was implemented in the '*rda*' function available in the '*vegan*' package for R (https://CRAN.R-project.org/package=vegan; http://R-project.org). GLM was implemented in the "*lm*" function available in '*stats*' package, and relative importance metrics for linear models were calculated in '*calc.relimp*' function available in the '*relaimpo*' package.[31] RDA is a direct gradient ordination analysis that summarizes linear relations between a set of response variables and explanatory variables.[33] We assessed multi-collinearities between the explanatory variables using a Spearman rank correlation matrixes and variance inflation factor (VIF) in R (the package '*corrplot*' and '*car*').[34] Highly correlated variables (i.e., R > 0.8 or VIF > 10) were removed from the subsequent analysis.

We further used the Random Forest (RF) algorithm[35] to reveal the non-linear relationships between the monitored DO concentrations (or ΔDO) and the other water quality indexes. RF is a machine learning algorithm used to fit a large ensemble of randomly assembled classification or regression trees to the bootstrapped samples of the response variables, and the outputs of these trees are averaged to produce the simulated response.[35,36] RF modeling is highly accurate, resistant to outliers, and good at handling complex interactions between the response and predictor variables.[36] RF includes the methods to quantify how these statistically derived models relate the input explanatory variable to produce the simulated responses.[36] Permutation importance describes the increases of the mean squared error (MSE) by the randomly permutating explanatory variables in out-of-bag sample. Partial dependence is a measure of an explanatory variable's influence on the response variable given the effects of all the other explanatory variables in the model and is calculated across ranges for observations of each explanatory variable. Permutation importance and partial dependence has been calculated by the '*partialPlot*' and '*varImpPlot*' functions in the '*randomForest*' package.[37]

RF algorithm was performed using the '*randomForest*' package. We conducted 10-fold cross-validation to fit and test the models by the following steps: (1) The water quality Dataset 2 with the lake monitoring stations in 2018 was randomly divided into 10 folds of approximately equal size; (2) RF model was divided into nine folds, the training dataset with the remaining fold being used to evaluate model performance. This procedure was repeated 10 times with a different fold treated as the testing dataset each time. Thus, a total of 10 models were developed in this study, and each forest had comprised 500 trees, and the parameter 'mtry' was set to '3'; (3) The permutation importance and partial dependence of all the explanatory variables for each model were tabulated to quantify relationships between ΔDO and each water quality index. Model performance was evaluated using the coefficient of determination (R^2) and root mean square error (RMSE), calculated between predicted and observed ΔDO.

RESULTS

Seasonal patterns of DO and ΔDO in lake surface

Our results highlight the seasonal variations of DO concentrations and the saturation status of lakes across China (Figures 2A-B). From winter to summer, around 65% of these surveyed lakes shifted from DO undersaturation to oversaturation (Figure 2C). Specifically, more than half of these lakes experienced DO oversaturation from April to September, while more than three quarters of the lakes showed DO undersaturation enduring from October to March (Figure 2C). Particularly in summer (from June to August), two thirds of these lakes showed DO oversaturation, with an average ΔDO of 0.91 (0.12–2.29) $mg \cdot L^{-1}$ (median and 95% confidence interval). By contrast, around 92% of all these investigated lakes exhibited DO undersaturation in winter, with an average ΔDO of -1.51 (-3.58 – -0.36) $mg \cdot L^{-1}$. Due to higher gas solubility at low water temperature in winter, both the saturated and measured DO concentrations in the lakes were higher in winter than in summer ($P < 0.01$, Student-*t* test). By contrast, ΔDO was typically higher in summer than in winter (Figure 2). We compared the characteristics of DO_{sat}, DO, and ΔDO trends between subtropical and temperate lakes (Figure S1). In general, no significant difference has been observed in ΔDO regardless of the seasons ($P > 0.1$). Additionally, the lakes of positive ΔDO values were always associated to the higher Chl-a concentration (i.e., 14.9 (2.3–71.6) $\mu g \cdot L^{-1}$) than those with negative ΔDO values (i.e., 5.6 (1.3–30.6) $\mu g \cdot L^{-1}$) ($P < 0.01$, Student-*t* test, Figure S2). Thus, our results highlight the potential importance of *in situ* oxygen productions through the photosynthesis of primary producers in regulating seasonal variations of lake DO.

Decadal increases of DO and ΔDO in China's lakes

Long-term monitoring data on a subset for 50 lakes from 2006–2018 demonstrated profound DO enrichment with significant increasing trend of both DO and ΔDO (Figures 3A-B). Due to lake warming, DO_{sat} has declined in 45 of the 50 lakes at a rate of -0.06 (-0.17–0.01) $mg \cdot L^{-1}$ per year, while DO concentration has increased in 34 out of 50 lakes at a rate of 0.02 (-0.17–0.27) $mg \cdot L^{-1}$ per year (Figure S3). Jointly, ΔDO had increased with an average rate of 0.07(-0.11–0.43) $mg \cdot L^{-1}$ per year during 2006–2018 ($P < 0.01$). Particularly, 39 lakes displayed an increasing trend of ΔDO (average rate: 0.17 $mg \cdot L^{-1}$ per year), while only 11 lakes presented a decreasing trend (average rate, -0.09 $mg \cdot L^{-1}$ per year, Figure 3A). We have divided these lakes into eutrophic, mesotrophic, and oligotrophic based on their annual average Chl-a concentrations.[38] From 2006 to 2018, we found significant differences

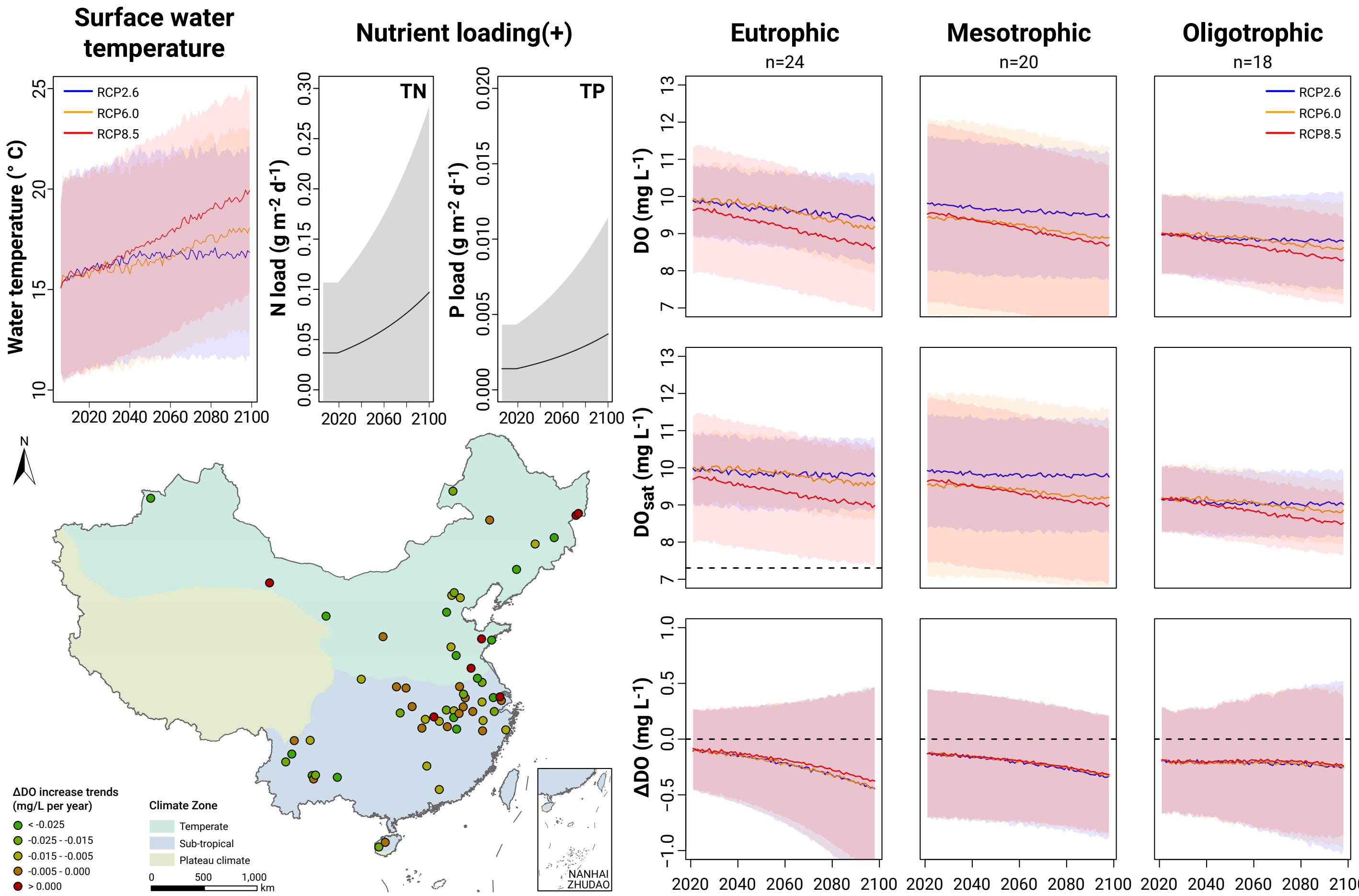

Figure 5. Future projections of DO_{sat}, DO, and ΔDO in lakes across China with distinct trophic states under the scenarios of climate warming (i.e., RCP 2.6/6.0/8.5) and nutrient loading increases TN and TP refer to the nutrient load of total nitrogen and total phosphorus, respectively.

among these three types of lakes in the DO change rates of 0.005, 0.001, and -0.006 mg·L^{-1} per year, and in the ΔDO change rate of 0.013, 0.008, and 0.001 mg·L^{-1} per year, respectively (Figure 3C). We also observed a positive relationship between the ΔDO and Chl-a trends during 2006–2018 ($P = 0.004$) (Figure S4). All these results indicated stronger long-term oxygen enrichment in more productive lakes. No significant difference was found on historical trends of DO and ΔDO for subtropical and temperate lakes ($P > 0.1$).

Drivers of the long-term oxygen enrichments in China's lakes

Multiple environmental factors can contribute to the variation of lake DO.[1,17] DO_{sat} is regulated by oxygen solubility depending on air pressure and water temperature.[17] In line with the rising air temperature (Figure S5), water temperature increased substantially in the 50 lakes with long-term observation with a median rate of 0.24 (-0.04–0.64)°C per decade from 2006–2018, which was consistent with the global median of 0.34 (0.16–0.52)°C per decade.[39] We found that water temperature increased in the lakes with rising air temperatures and declining wind speeds, and the former leading to a declining DO_{sat}. By contrast, most lakes have experienced increasing DO (Figure S6) , diverging from patterns reported in both temperate[1] and global lakes.[9] The trend of DO deviates from those of DO_{sat} ($P > 0.1$; Figure S6). Specifically, 31 out of 50 lakes with a rising DO exhibit decreased DO_{sat}. These results indicate that declining oxygen solubility may have limited influence on the long-term trends of lake DO in China.

Our modeling results suggest that for all the lakes on an annual average scale, GPP was the dominant input flux of DO (Figure 4). Contribution of phytoplankton growth to GPP represents 82.5 (43.4–99.8)%, and it is more dominant in the eutrophic and mesotrophic lakes (99.1 [91.6– 99.8]%) (the rest from macrophytes). In autumn and winter, reaeration become another source of the lake DO (39.2%). For DO sinks, seasonal patterns emerge such that EC represents 53.3% followed by diffusive outgassing (46.7%) due to the oversaturation in spring and summer, while in autumn and winter, EC dominates the total DO output (Figure 4). In general, DO fluxes were much higher in eutrophic lakes than the mesotrophic or oligotrophic lakes: 2.06 (1.75–2.29) and 3.12 (2.64–3.34) times higher in eutrophic lakes compared to mesotrophic and oligotrophic lakes, respectively. Furthermore, this model unraveled a significant increasing trend of GPP (GPP_P, from phytoplankton) over the entire simulated period in eutrophic lakes, which resulted in an increasing and positive NEP, suggesting increased net productivity (Figure 4). Taken together, the process-based modeling indicated that increasing GPP (and NEP) was the dominant driver of the increasing lake DO, particularly in the eutrophic lakes during warmer seasons. Combined with the warming-driven reduced DO_{sat}, ΔDO kept increasing over the study period from 2006 to 2018.

We further validate our results using data-driven analysis. We identified the long-term trends of water temperature, Chl-a (representing GPP), COD_{Mn} (representing EC), and nutrient concentrations (i.e., TN and TP) together with DO and DO_{sat} (Figures S7-S8). We found that Chl-a concentration had increased in 32 of the 50 lakes with a median rate of 0.16 μg·L^{-1} per year, which was in concert with global trends[11,12] and potentially related to the lake warming as reflected by the positive relationships between the rates of water warming and Chl-a increase ($P < 0.01$, Figure S9). A general linear model (GLM)[31] further showed that increased DO and ΔDO were mainly correlated to the increasing Chl-a concentration, accounting for 63% and 53% of the variations, respectively (Table 1). We found that the more productive lakes (i.e. Chl-a > 8 μg·L^{-1})[38] showed a higher ΔDO than the less-productive lake ($P < 0.01$, Student's t test, Figure S10). These results coincide with the projections of PCLake+ modeling and together confirm the critical role of increasing GPP (via phytoplankton growth and hence Chl-a) in driving the increasing DO and ΔDO values. Significantly, the observed positive correlation between the increasing ΔDO and enhanced water temperature ($P < 0.01$) contradicted the

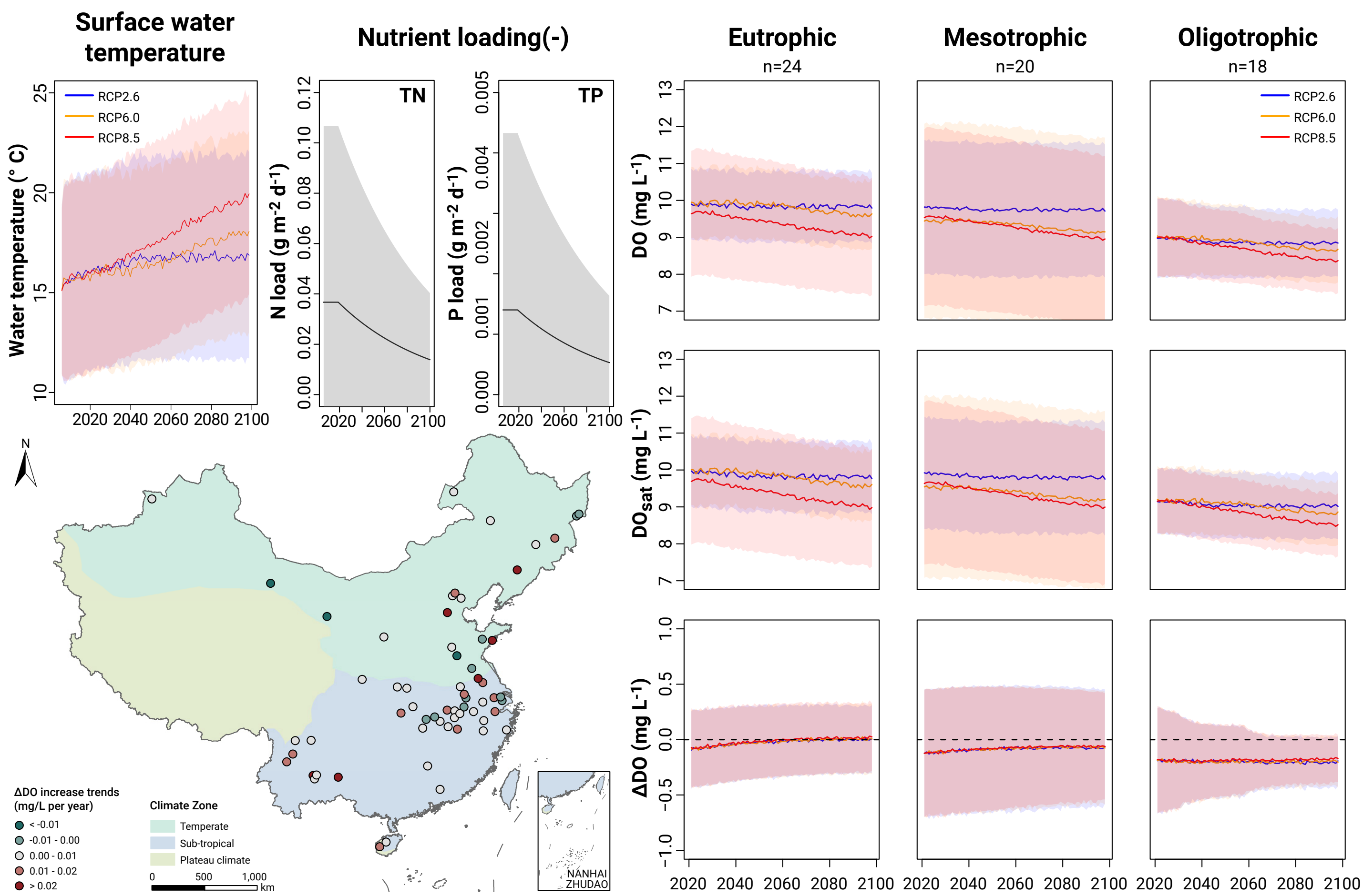

Figure 6. Future projections of DO_{sat}, DO, and ΔDO in lakes across China with distinct trophic states under the scenarios of climate warming (i.e., RCP 2.6/6.0/8.5) and nutrient loading decreases TN and TP refer to the nutrient load of total nitrogen and total phosphorus, respectively.

previous findings for temperate lakes.[1,10] The contrasting relationships probably imply a complementary pattern only representing the initial stage of eutrophication in China's lakes emphasizing a positive impact of Chl-a concentration on the DO ($P < 0.01$, Figure S11).

Projections of DO and ΔDO under intensified nutrient inputs and climate warming

We utilized the PCLake model to predict the future dynamics of DO and ΔDO in China's lakes. Three climate warming schemes (i.e., RCP2.6/6.0/8.5) and two nutrient loading scenarios (i.e., nutrient (+) and nutrient (-)) are designed, which lead to six scenarios for each lake from 2020 to 2099 (Figures 5-6). Based on the nutrient loading change rates for China's lakes during 2006–2018,[31,32] nutrient loading changes at a realistic rate of ±0.1% per month from 2019 to 2099, leading to either a total reduction of -62.3% (nutrient (-)) and +264% increase (nutrient (+)) (see MATERIALS AND METHODS).

Under the nutrient (+) scenario, our model predicts that lake warming would drive a long-term, gradual decline in DO_{sat}, with a faster rate under the more intense warming scenario (RCP8.5). Moreover, the model projects a consistent decline in DO across all scenarios and lake trophic groups, with a greater magnitude of decline under more intense warming scenarios. Collectively, ΔDO decreased and diverged further from DO saturation across all lake trophic groups, with the most pronounced deviations observed in eutrophic lakes. Meanwhile, climate warming induced only marginal differences in ΔDO across RCP scenarios, and ΔDO trends were consistent across seasons (Figure S12). Our models further revealed that shifts in metabolic balance (net ecosystem production, NEP) govern future ΔDO patterns. On an annual scale, the decline in ΔDO can be attributed to asymmetric increases in gross primary production (GPP) and ecosystem respiration (EC)—with EC increasing more rapidly than GPP—and the transition from positive to negative NEP, which drives deoxygenation (Figure S13). Our modeling further demonstrates that, for eutrophic lakes, the rate of ΔDO change did not differ between temperate and subtropical systems, whereas temperate lakes exhibited a higher absolute ΔDO value (Figure S14). Conversely, under the nutrient (-) scenario, ΔDO remains stable or even increases to exceed zero (DO saturation) across all lake groups and RCP scenarios—indicating that surface lake DO would be preserved under a nutrient reduction regime, regardless of climate warming intensity. Over, these model projections therefore indicate that the current surface oxygen enrichment in China's lakes is likely a transient state, contingent on future climate and nutrient loading regimes.

DISCUSSION

Despite widespread deoxygenation observed in global lakes[8,9] with a dominant downward trend (83% of lakes, -0.049 $mg \cdot L^{-1} \cdot decade^{-1}$) driven by climate warming (55% contribution) and heatwaves, we reveal a widespread DO enrichment in China's lakes, particularly in the eutrophic lakes based on a comprehensive and long-term monitoring dataset (Figures 2-3). Our results suggest that this discrepancy reflects regional heterogeneity in lake DO responses, mainly attributable to the nutrient enrichment driven by intensive anthropogenic interventions and algal-induced DO increases that outweigh warming-induced DO solubility decline in our study area. Compared to the ongoing effort in the developing countries in Southeast Asia, Africa, and South America, water eutrophication control measures were implemented much earlier in developed countries, for example, the Clean Water Act in the US in 1972.[14,40] As a result, water quality issues tend to be more severe in the developing countries due to the persistently high N and P concentrations.[13,14,32,40] Since the 2000s, China has initiated massive efforts to reduce particularly point-source N and P inputs into lakes.[31] In response, the average national P concentration in the lakes has progressively declined (down to ~60 $\mu g \cdot L^{-1}$) but remains higher than the lake in the US (~20–40 $\mu g \cdot L^{-1}$) and Europe

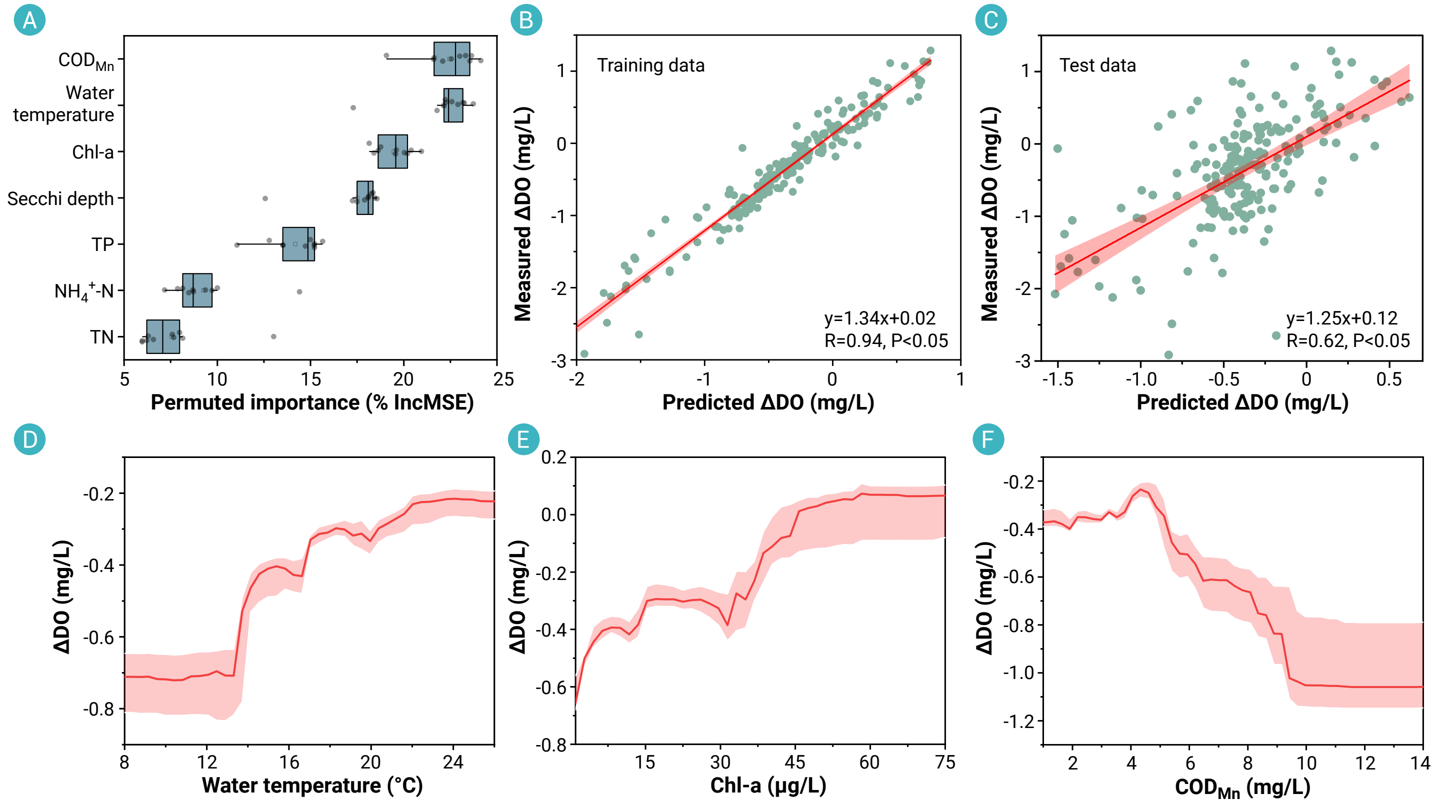

Figure 7. Random Forests models of DO saturation in 101 lakes in 2018. A total of 10 Random Forest models were developed corresponding to 10-fold cross-validation (A) Permuted importance of explanatory variables. X-axes are % change in mean squared error (MSE); (B and C) model performance when tested against training and testing sets; (D-F) partial dependence plots of lake ΔDO on water temperature, Chl-a, and COD_{Mn}. Solid line represents the median of the 10 models, and the shaded areas are bound by min. and max. partial dependences.

(~25 μg·L^{-1}).[41,42] Moreover, they are still above the threshold of the algal blooms (20 μg·L^{-1}),[40] leading to the persistent occurrences of algal blooms and increasing Chl-a concentrations in many lakes.[43] Thus, our results complement the global deoxygenation narrative by highlighting context-dependent lake responses, enhancing the understanding of global lake DO dynamics.

Notably, spatial heterogeneity in lake oxygen dynamics resolves the discrepancy between our finding of surface DO increase (driven by eutrophication) and the well-documented eutrophication-induced bottom hypoxia.[44] Eutrophication elevates surface DO via enhanced algal photosynthesis yet triggers benthic hypoxia through microbial decomposition of sinking organic detritus. Here, bottom hypoxia is intensified often by thermal-induced stratification which limits the vertical replenishment of DO in deeper water layers.[45] This distinction underscores the critical need to clarify the spatial scope of lake DO trends, such that eutrophication exerts vertically uneven effects on lake DO, directly informing nutrient reduction strategies that preserve surface DO while mitigating benthic hypoxia to balance aquatic ecosystem health.

In addition, it is widely recognized that ongoing climate warming drives two key lake responses, i.e. promoting primary production[12] and reducing dissolved oxygen (DO) solubility.[1] The stimulatory effect on primary production is supported by both single-lake case studies[19] and latitudinal gradient comparisons.[46] For reduced DO solubility based on an estimated lake water warming rate of 0.34 [0.19–0.48]°C per decade,[39] freshwater lakes (at 15°C) could experience a DO_{sat} decline of ~0.03–0.11 mg·L^{-1} per decade. However, lake warming simultaneously stimulates phytoplankton growth: a 0.10°C temperature rise is associated with a ~0.21 μg·L^{-1} Chl-a increase (Figure S9). Assuming an organic C:Chl-a mass ratio of 40, the Chl-a boost (~0.71 μg·L^{-1}, matching a 0.34°C warming rate) would drive a ~0.07 mg·L^{-1} DO increase via photosynthesis, an effect comparable in magnitude to the DO_{sat} decline from warming. Further, our Random Forest model revealed that ΔDO (DO trend) remains stable at ~−0.7 mg·L^{-1} below 15°C, rises as temperatures increase from 15°C to 25°C (Figure 7), and plateaus above 25°C despite further warming. This pattern aligns with the typical optimal growth temperature for phytoplankton (~20°C).[47] Thus, unlike eutrophication that directly amplifies surface oxygen production via nutrient-fueled algal growth, the modest photosynthetic benefits by lake warming are likely offset by the concurrent reduction in water's oxygen solubility.

Future projections suggest that increased nutrient loading may reverse DO enrichment in a warmer climate and lead to deoxygenation (Figure 5). First, based on the process-based PCLake+ model projections, we have explicitly partitioned the relative contributions of temperature-driven oxygen solubility changes and biological/ecological processes (e.g., photosynthesis, respiration) to projected surface DO dynamics under nutrient (+). Results show that reduced oxygen solubility accounts for 15%–22% of the projected surface DO variation under warming alone, while biological processes including oxygen production (GPP) and consumption (EC) dominate the remaining 78%–85% of changes. Then, we show that despite enhanced GPP due to increasing nutrient loads, higher oxygen consumptions (EC, e.g., respiration, mineralization) could offset the higher DO production, resulting in decline of NEP and eventually promoting oxygen depletion (Figure S13). Ecosystem metabolism shows asymmetric sensitivities to water temperature. While both GPP and ER increase with temperature, ER exhibits a stronger response (Q_{10} = 2.3 vs. GPP Q_{10} = 1.8), leading to a progressive decline in net oxygen production (GPP - ER) under sustained warming, such that 1°C warming would lead to a 23.6% higher increase in EC than in GPP[18] and shift between autotrophy and heterotrophy is water-temperature dependent.[48] This metabolic imbalance is exacerbated by (1) increased mineralization of organic matter under higher temperatures, and (2) photoinhibition at elevated temperatures limiting phytoplankton productivity. The tipping point occurs when cumulative EC exceeds GPP, triggering a shift from net oxygen production to consumption, a transition observed in our model simulations at ~3.5°C above baseline conditions. Therefore, climate warming could further amplify the lake DO deoxygenation, particularly in more eutrophic lakes.[46] The projected findings presented in this study are applicable to the warm lakes such as those found in China and Florida. However, it is important to note that contrasting results have been observed in the cold and temperate Danish lakes where nutrient loading has reported a different influence on DO concentration probably because they are mostly under low nutrient levels representing a restoration phase of eutrophication.[46]

Anchoring our future scenarios to observed historical dynamics (2006–2018) strengthens the interpretability of model outputs. The balance between solubility-driven oxygen loss and nutrient-modulated biological oxygen production will remain a central driver of lake deoxygenation under future warming. This historical context underscores that future DO responses depend on the interplay between physical solubility effects and ecological processes, emphasizing the need for combining nutrient management with climate mitigation to safeguard lake oxygen status.

Our findings underscore the significance of maintaining a metabolic balance between lake DO production and consumption, as well as intricate relationships between climate warming and eutrophication when predicting lake DO levels. These factors have contributed to the recent DO enrichments observed in numerous lakes in China. However, we anticipate that such oxygen enrichment could be reversed in a warmer future if nutrient loads continue to increase. To mitigate potential risks of lake deoxygenation, it is crucial to implement nutrient reduction measures that not only focus on controlling algal bloom (measured by Chl-a concentration) but also prioritize the sustainability of lake DO levels (measured by ΔDO). A DO-guided nutrient reduction strategy should be developed in the future lake eutrophication control. It is important to recognize that the relationship between lake eutrophication and DO levels is intricate. While an increase in primary production could elevate lake DO level through intensified photosynthesis, a significant increase in organic carbon could accelerate the consumption of DO. In recent decades, nutrient reductions have proven to be an effective strategy in mitigating eutrophication, as evidenced by the successful cases in Europe and the US. However, our research underscores the critical importance of assessing the potential impact on DO change in lakes before implementing any actions. This consideration is especially crucial due to the pivotal role of DO in sustaining overall health and balance of aquatic ecosystems.

A key limitation of this study lies in the scope of our oxygen data and the exclusion of specific lake processes, which should be contextualized alongside prior research. While a previous study on temperate lakes[1] quantified whole-lake oxygen budgets using depth-integrated measurements, our focus on surface data enables the capture of photic zone dynamics (e.g., primary production, gas exchange) but does not resolve deep-water hypoxia as a critical component of lake deoxygenation. Additionally, although winter ice cover is rare in our set of lakes, the exclusion of ice-related biogeochemical processes remains a limitation, given the well-documented regulatory role of lake ice in DO dynamics. These biogeographical and methodological differences highlight the need for caution when interpreting drivers of lake deoxygenation, as findings are context dependent. Future studies should integrate under-ice monitoring and vertical hydrodynamic data to more comprehensively characterize climate-driven oxygen shifts across the entire water column.

Overall, contrary to widespread lake deoxygenation globally, long-term observations (> 10 years) from nearly 100 Chinese lakes reveal significant oxygen enrichment in surface waters. Our integrated analysis combining data-driven approaches and process-based modeling demonstrates that this enrichment is driven primarily by eutrophication-induced primary production. However, this trend appears unsustainable under climate warming, as rising oxygen consumption increasingly outpaces production. These findings establish distinct lake oxygen dynamics under varying climatic and trophic conditions and underscore that current oxygen gains in China's lakes do not ensure long-term resilience. For the studied lakes, deoxygenation is likely if eutrophication intensifies and management strategies continue to lack targeted oxygen conservation measures (e.g., nutrient management oriented to oxygen balance, aeration equipment deployment). In contrast, effective oxygen conservation management is expected to mitigate or even avoid such deoxygenation risks, as demonstrated in many successful lake management cases.

REFERENCES

1. Jane S. F., Hansen G. J. A., Kraemer B. M., et al. (2021). Widespread deoxygenation of temperate lakes. *Nature* **594**:66–70. DOI:10.1038/s41586-021-03550-y
2. North R. P., North R. L., Livingstone D. M., et al. (2014). Long-term changes in hypoxia and soluble reactive phosphorus in the hypolimnion of a large temperate lake: Consequences of a climate regime shift. *Glob. Change Biol.* **20**:811–823. DOI:10.1111/gcb.12371
3. Fernandez J. E., Peeters F. and Hofmann H. (2014). Importance of the autumn overturn and anoxic conditions in the hypolimnion for the annual methane emissions from a temperate lake. *Environ. Sci. Technol.* **48**:7297–7304. DOI:10.1021/es4056164
4. Michalak A. M., Anderson E. J., Beletsky D., et al. (2013). Record-setting algal bloom in Lake Erie caused by agricultural and meteorological trends consistent with expected future conditions. *Proc. Natl. Acad. Sci. USA* **110**:6448–6452. DOI:10.1073/pnas.1216006110
5. Harke M. J., Steffen M. M., Gobler C. J., et al. (2016). A review of the global ecology, genomics, and biogeography of the toxic cyanobacterium, Microcystis spp. *Harmful Algae* **54**:4–20. DOI:10.1016/j.hal.2015.12.007
6. Tong Y., Feng L., Wang X. C., et al. (2023). Global lakes are warming slower than surface air temperature due to accelerated evaporation. *Nat. Water* **1**:929–940. DOI:10.1038/s44221-023-00148-8
7. Piccolroaz S., Zhu S., Ladwig R., et al. (2024). Lake water temperature modeling in an Era of climate change: Data sources, models, and future prospects. *Rev. Geophys.* **62**:e2023RG000816. DOI:10.1029/2023RG000816
8. Jansen J., Simpson G. L., Weyhenmeyer G. A., et al. (2024). Climate-driven deoxygenation of northern lakes. *Nat. Clim. Chang.* **14**:832–838. DOI:10.1038/s41558-024-02058-3
9. Zhang Y., Shi K., Woolway R. I., et al. (2025). Climate warming and heatwaves accelerate global lake deoxygenation. *Sci. Adv.* **11**:eadt5369. DOI:10.1126/sciadv.adt5369
10. Breitburg D., Levin L. A., Oschlies A., et al. (2018). Declining oxygen in the global ocean and coastal waters. *Science* **359**:46–56. DOI:10.1126/science.aam7240
11. Ho J. C., Michalak A. M. and Pahlevan N. (2019). Widespread global increase in intense lake phytoplankton blooms since the 1980s. *Nature* **574**:667–670. DOI:10.1038/s41586-019-1648-7
12. Meerhoff M., Audet J., Davidson T. A., et al. (2022). Feedback between climate change and eutrophication: Revisiting the allied attack concept and how to strike back. *Inland Waters* **12**:187–204. DOI:10.1080/20442041.2022.2029317
13. Hou X. J., Feng L., Dai Y. H., et al. (2022). Global mapping reveals increase in lacustrine algal blooms over the past decade. *Nat. Geosci.* **15**:130–134. DOI:10.1038/s41561-021-00887-x
14. Jenny J. P., Anneville O., Arnaud F., et al. (2020). Scientists' warning to humanity: Rapid degradation of the world's large lakes. *J. Great Lakes Res.* **46**:686–702. DOI:10.1016/j.jglr.2020.05.006
15. Saravani M. J., Noori R., Jun C., et al. (2025). Predicting Chlorophyll-a concentrations in the world's largest lakes using Kolmogorov-Arnold networks. *Environ. Sci. Technol.* **59**:1801–1810. DOI:10.1021/acs.est.4c11113
16. Naderian D., Noori R., Kim D., et al. (2025). Environmental controls on the conversion of nutrients to chlorophyll in lakes. *Water Res.* **274**:123094. DOI:10.1016/j.watres.2025.123094
17. Marcé R., Gómez-Gener L. and Carey C. C. (2024). Chapter 11 - Oxygen. In Wetzel's Limnology (Fourth Edition), I.D. Jones, and J.P. Smol (eds). (Academic Press), pp:237-274. DOI:10.1016/B978-0-12-822701-5.00011-2
18. Song C., Dodds W. K., Rüegg J., et al. (2018). Continental-scale decrease in net primary productivity in streams due to climate warming. *Nat. Geosci.* **11**:415–420. DOI:10.1038/s41561-018-0125-5
19. Tong Y. D., Xu X. W., Qi M., et al. (2021). Lake warming intensifies the seasonal pattern of internal nutrient cycling in the eutrophic lake and potential impacts on algal blooms. *Water Res.* **188**:116570. DOI:10.1016/j.watres.2020.116570
20. CNEMC (2024). China national environmental monitoring centre. https://www.cnemc.cn
21. Huang W., Ma C., Li W., et al. (2021). Spatial-temporal variations of dissolved oxygen and their response to global warming in China. *Acta Sci. Circumst.* **41**:1970–1980 (in Chinese). DOI:10.13671/j.hjkxxb.2020.0330
22. Messager M. L., Lehner B., Grill G., et al. (2016). Estimating the volume and age of water stored in global lakes using a geo-statistical approach. *Nat. Commun.* **7**:13603. DOI:10.1038/ncomms13603
23. Hersbach H., Bell B., Berrisford P., et al. (2020). The ERA5 global reanalysis. *Q. J. R. Meteorol. Soc.* **146**:1999–2049. DOI:10.1002/qj.3803
24. MEPC (2014). Water quality-determination of total nitrogen by flow injection analysis (FIA) and N-(1-Naphthyl)ethylene diamine dihydrochloride spectrophotometry, (HJ668-2013). Ministry of Environmental Protection of China. https://www.mee.gov.cn/ywgz/fgbz/bz/bzwb/jcffbz/201311/W020131106589119080353.pdf
25. Janssen A. B. G., Teurlincx S., Beusen A. H. W., et al. (2019). PCLake+: A process-based ecological model to assess the trophic state of stratified and non-stratified freshwater lakes worldwide. *Ecol. Model.* **396**:23–32. DOI:10.1016/j.ecolmodel.2019.01.006
26. Kong X. Z., He Q. S., Yang B., et al. (2017). Hydrological regulation drives regime shifts: Evidence from paleolimnology and ecosystem modeling of a large shallow Chinese

lake. *Glob. Change Biol.* 23:737–754. DOI:10.1111/gcb.13416
27. Janse J. H., Scheffer M., Lijklema L., et al. (2010). Estimating the critical phosphorus loading of shallow lakes with the ecosystem model PCLake: Sensitivity, calibration and uncertainty. *Ecol. Model.* 221:654–665. DOI:10.1016/j.ecolmodel.2009.07.023
28. Nielsen A., Trolle D., Bjerring R., et al. (2014). Effects of climate and nutrient load on the water quality of shallow lakes assessed through ensemble runs by PCLake. *Ecol. Appl.* 24:1926–1944. DOI:10.1890/13-0790.1
29. Janssen A. B., de Jager V. C., Janse J. H., et al. (2017). Spatial identification of critical nutrient loads of large shallow lakes: Implications for Lake Taihu (China). *Water Res.* 119:276–287. DOI:10.1016/j.watres.2017.04.045
30. Harrison J. A., Maranger R. J., Alexander R. B., et al. (2009). The regional and global significance of nitrogen removal in lakes and reservoirs. *Biogeochemistry* 93:143–157. DOI:10.1007/s10533-008-9272-x
31. Tong Y. D., Wang M. Z., Penuelas J., et al. (2020). Improvement in municipal wastewater treatment alters lake nitrogen to phosphorus ratios in populated regions. *Proc. Natl. Acad. Sci. USA* 117:11566–11572. DOI:10.1073/pnas.1920759117
32. Tong Y. D., Zhang W., Wang X. J., et al. (2017). Decline in Chinese lake phosphorus concentration accompanied by shift in sources since 2006. *Nat. Geosci.* 10:507–511. DOI:10.1038/ngeo2967
33. Mahdiyan O., Filazzola A., Molot L. A., et al. (2021). Drivers of water quality changes within the Laurentian Great Lakes region over the past 40 years. *Limnol. Oceanogr.* 66:237–254. DOI:10.1002/lno.11600
34. Friendly M. (2002). Corrgrams: Exploratory displays for correlation matrices. *Am. Stat.* 56:316–324. DOI:10.1198/000313002533
35. Breiman L. (2001). Random forests. *Mach. Learn.* 45:5–32. DOI:10.1023/A:1010933404324
36. Nelson N. G., Munoz-Carpena R., Phlips E. J., et al. (2018). Revealing biotic and abiotic controls of harmful algal blooms in a shallow subtropical lake through statistical machine learning. *Environ. Sci. Technol.* 52:3527–3535. DOI:10.1021/acs.est.7b05884
37. Tong Y. D., Xu X. W., Zhang S. L., et al. (2019). Establishment of season-specific nutrient thresholds and analyses of the effects of nutrient management in eutrophic lakes through statistical machine learning. *J. Hydrol.* 578:124079. DOI:10.1016/j.jhydrol.2019.124079
38. OECD (1982). Eutrophication of waters: Monitoring, assessment and control. Paris: OECD. https://www.oecd.org/env/outreach/30693798.pdf
39. O'Reilly C. M., Sharma S., Gray D. K., et al. (2015). Rapid and highly variable warming of lake surface waters around the globe. *Geophys. Res. Lett.* 42:10773–10781. DOI:10.1002/2015GL066235
40. Tong Y. D., Huang Z., He W., et al. (2022). Influence of social and environmental drivers on nutrient concentrations and ratios in lakes: A comparison between China and Europe. *Water Res.* 227:119347. DOI:10.1016/j.watres.2022.119347
41. European Environment Agency (2018). European waters – Assessment of status and pressures 2018. EEA Report No 7/2018. Luxembourg: European Environment Agency. DOI:10.2800/63266
42. U.S. Environmental Protection Agency (2022). National lakes assessment: The third collaborative survey of lakes in the United States. Washington, DC: U.S. Environmental Protection Agency. DOI:10.23719/1531936
43. Ma J. E., Loiselle S., Cao Z. G., et al. (2023). Unbalanced impacts of nature and nurture factors on the phenology, area and intensity of algal blooms in global large lakes: MODIS observations. *Sci. Total Environ.* 880:163376. DOI:10.1016/j.scitotenv.2023.163376
44. Lewis A. S., Lau M. P., Jane S. F., et al. (2024). Anoxia begets anoxia: A positive feedback to the deoxygenation of temperate lakes. *Glob. Change Biol.* 30:e17046. DOI:10.1111/gcb.17046
45. Ladwig R., Hanson P. C., Dugan H. A., et al. (2021). Lake thermal structure drives interannual variability in summer anoxia dynamics in a eutrophic lake over 37 years. *Hydrol. Earth Syst. Sci.* 25:1009–1032. DOI:10.5194/hess-25-1009-2021
46. Jeppesen E., Canfield D. E., Bachmann R. W., et al. (2020). Toward predicting climate change effects on lakes: A comparison of 1656 shallow lakes from Florida and Denmark reveals substantial differences in nutrient dynamics, metabolism, trophic structure, and top-down control. *Inland Waters* 10:197–211. DOI:10.1080/20442041.2020.1711681
47. Huisman J., Codd G. A., Paerl H. W., et al. (2018). Cyanobacterial blooms. *Nat. Rev. Microbiol.* 16:471–483. DOI:10.1038/s41579-018-0040-1
48. Scharfenberger U., Jeppesen E., Beklioglu M., et al. (2019). Effects of trophic status, water level, and temperature on shallow lake metabolism and metabolic balance: A standardized pan-European mesocosm experiment. *Limnol. Oceanogr.* 64:616–631. DOI:10.1002/lno.11064

FUNDING AND ACKNOWLEDGMENTS

This study was supported by the National Natural Science Foundation of China (U24A20640, 42377399, and 42177062), the Science and Technology Projects of Xizang Autonomous Region, China (XZ202502JD0025, XZ202502ZY0019, XZ202501ZY0091), the National Key Research and Development Program of China (2023YFF0807203), Science and Technology Planning Project of NIGLAS (NIGLAS2022GS02, NIGLAS2022GS09), Key Laboratory of Lake and Watershed Science for Water Security (NKL2023-ZD02, NKL2023-KP02), and International Partnership Program of Chinese Academy of Sciences (IPP) (045GJHZ2023055FN). YD Tong was supported by distinguished professor project in Tibet University. E Jeppesen was supported by the TÜBITAK program BIDEB2232 (118C250). XK was supported by the "Hundred People Program" of the Chinese Academy of Sciences. The funders had no role in study design, data collection and analysis, decision to publish, or preparation of the manuscript. We thank Anne Mette Poulsen for valuable English editions.

DECLARATION OF INTERESTS

Erik Jeppesen is an Editorial Board member of The Innovation Geoscience and was blinded from reviewing or making final decisions on the manuscript. Peer review was handled independently of this member and their research group. The other authors declare no conflicts of interest.

DATA AND CODE AVAILABILITY

All the data supporting the present study are available in the following Zenodo repository: https://doi.org/10.5281/zenodo.13377650.

SUPPLEMENTAL INFORMATION

It can be found online at https://doi.org/10.59717/j.xinn-geo.2026.100215.